Journal of Applied Fluid Mechanics, Vol. 14, No. 5, pp. 1351-1362, 2021.
Available online at www.jafmonline.net, ISSN 1735-3572, EISSN 1735-3645.
https://doi.org/10.47176/jafm.14.05.32163

Heat Transfer and Hydraulic Characteristics of Supercritical CO_2 in Cooled and Heated Horizontal Semicircular Channels

Y. Tu [1†] and Y. Zeng [2]

[1] *Hunan University of Arts and Science, Changde, Hunan, 415000, China*
[2] *Beihang University, Beijing; 100191, China*

†*Corresponding Author Email: tuyi.huas@outlook.com*

(Received September 3, 2020; accepted March 27, 2021)

ABSTRACT

Heat transfer characteristics of supercritical CO_2 in horizontal semicircular channels are numerically investigated using Computational Fluid Dynamics method validated with experimental data. Comparison study is conducted for semicircular and circular channels with the same hydraulic diameter and boundary condition at the bulk temperature range including pseudocritical point. The results show that the heat transfer coefficients of the semicircular channel are significantly smaller than those of the circular channels due to the blocking effect at the corner area of the channel cross section, and the fluid thermophysical properties near the wall have a significant effect on the convective heat transfer performance in both heating and cooling cases. A modified model was proposed based on Olson correlation of the semicircular channel considering the channel geometry and near-wall fluid viscosity influence. Further study was conducted to discuss the effect of hydraulic diameter and boundary conditions on the heat transfer performance of the semicircular channel and indicate that the modified correlation shows a reasonable prediction of the heat transfer coefficients in the heated semicircular channel.

Keywords: Microchannel; Supercritical CO_2; Heat transfer; Semicircular channel; Computational fluid dynamics.

NOMENCLATURE

a	area
b	bulk
C_p	specific heat
d	hydraulic diameter
f	friction factor
g	mass flux
h	heat transfer coefficient
i	specific enthalpy
k	thermal conductivity
L	length
m	pseudocritical
Nu	Nusselt number
P	pressure
Pr	Prandtl number
q	heat flux
Re	Reynolds number
t	temperature
v	velocity
w	wall
μ	dynamic viscosity
ρ	density

1. INTRODUCTION

Carbon dioxide behaves as a supercritical fluid above its critical temperature (304.25 K) and critical pressure (7.39 MPa), in this condition it has unique thermal properties with enhanced heat transfer and flow characteristics (Rao *et al.* 2016). As shown in Fig.1. The large specific heat capacity near the pseudocritical point can greatly improve the capability of supercritical carbon dioxide (SCO_2) for heat transfer enhancement. In addition, CO_2 is a nontoxic, non-flammable, and inexpensive natural refrigerant which has been applied to automobile air conditioners, hot-water supplies, and gas turbine reactors (Kim *et al.* 2015). PCHE (Print Cycle Heat Exchanger) is categorized as a plate-fin type compact heat exchanger with high robustness for high-temperature, high-pressure applications and high compactness (Chen *et al.* 2016). It exhibits potential applications in the field of next generation nuclear power, solar thermal power generation, and hydrogen energy. The flow channels of PCHE are produced by chemical etching on flat metal plates with millimeter-level hydraulic diameter, and its main channel cross-section in industrial manufacturing recently is semicircular (Kim *et al.* 2010)(Tsuzuki *et al.* 2007). Studying the hydraulic and heat transfer characteristics of SCO_2 fluid in semicircular cross section microchannels is of great significance for the design and application of SCO_2 fluid PCHE.

Most of the existing researches on the flow and heat transfer characteristics of supercritical fluid channels focused on circular channels. Empirical correlations were set up based on a series of experimental and numerical studies for various pipe diameters, different fluid types, wide temperature, and Re range, which are summarized by (Pitla *et al.* 1999) and (Cabeza *et al.* 2017).

For the heat transfer and flow performance of the semicircular channel, most of the studies are conducted as part of the PCHE. (Figley *et al.* 2013) and (Mylavarapu *et al.* 2009) did numerical and experimental studies for circular and semicircular channels with helium as the working fluid. (Nikitin *et al.* 2006) studied the heat transfer and pressure drop characteristics of zigzag channels PCHE with semicircular cross section in SCO_2 experimental loop. (Meshram *et al.* 2016) evaluated the performance of a PCHE with straight and zigzag channels in fully turbulent conditions numerically and found that the channel diameter and the operating Reynolds number play significant roles in the overall heat transfer and pressure drop of hot and cold channels of SCO_2. (Kruizenga *et al.* 2012) performed a comparison between computational fluid dynamics analysis and experimental results for horizontal semicircular channels and found that the heat transfer results were well predicted by FLUENT.

Although several studies on the heat transfer performance of PCHE channels have been reported, little knowledge is available for the difference of the flow and heat transfer characteristics between

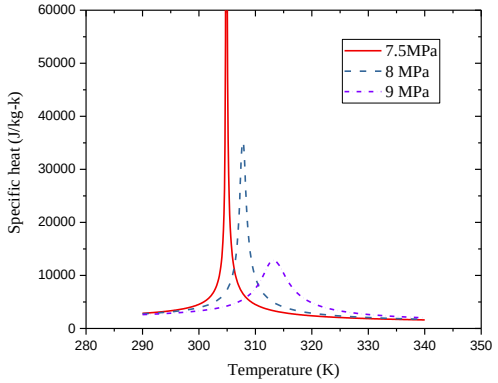

(a) Specific heat

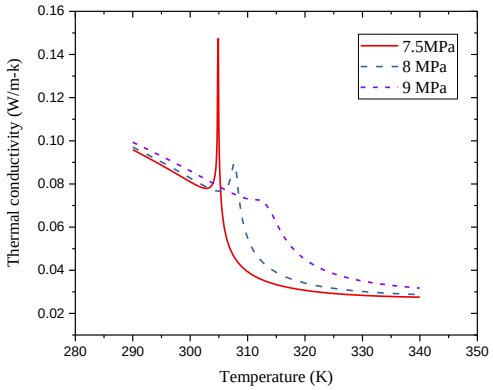

(b) Thermal conductivity

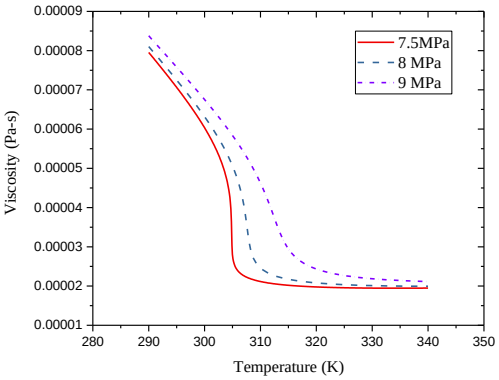

(c) Dynamic viscosity

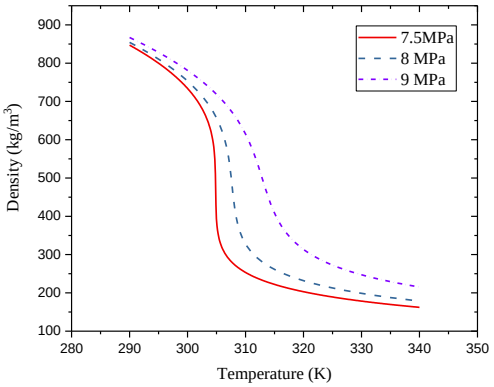

(d) Density

Fig. 1. Thermo-physical properties of CO_2 at 7.5, 8.0, and 9MPa.

circular and semicircular channels, and for telling the applicability of the correlations between circular channels and semicircular channels. There is still lacking of a generalized model to predict the heat transfer coefficients of supercritical CO_2 in semicircular channels. The current work uses supercritical CO_2 as the fluid medium to study its flow and heat transfer characteristics in the horizontal semicircular channel with CFD method verified by experimental data.

2. RESEARCH OBJECT

The research objects are the circular and semicircular straight channels including diameter 10.922 mm and 6 mm circular pipe for model validation analysis, and diameter 6 mm, 4 mm, 2 mm semicircular tubes for the hydraulic and heat transfer characteristics study. The analyses were carried out at constant mass flow inlet conditions. The inlet mass flow ranges from 200 to 600 kg/m^2-s and the bulk temperature ranges from 290 K to 340 K. The pressure outlet is adopted in this analysis with average pressure 7.5MPa, 8 MPa and 9 MPa. The wall surface of the cooling or heating section adopts a constant heat flux ranging from -18 kW/m^2 to 18 kW/m^2.

3. MODEL VALIDATION

3.1 Validation model description

In this paper, the experimental models of Dang (Dang and Hihara 2004) and Olson (Douglas and Olson 1998) are used as the validation models of circular channel for cooling and heating process. The experimental model of Li (Li *et al.* 2016) is used as the validation model of the semicircular channel for cooling and heating process.

3.2 Numerical method and model setup

ANSYS FLUENT 2019 R2, the commercially available CFD software, was employed in this numerical analysis. SST k-omega model is opted for modeling turbulence. Although k-omega model has higher accuracy as the wall function is not used in this modelling, it also leads to the difficulty of convergence and sensitivity to initial conditions, especially for SCO_2 fluid, the thermophysical properties of which change dramatically, making the model convergence more difficult. On the contrary, the k-epsilon model based on the wall function can improve the convergence and mesh requirements, but it will sacrifice the simulation accuracy. The SST model combines the advantages of the k-omega and k-epsilon models using blending functions, in which the k-omega model is activated in the near-wall region, and the k-epsilon model is used in the region far from the wall.

This model has been verified and applied in the numerical simulation of supercritical CO_2 channel internal flow in (Li *et al.* 2011) and (Lee and Kim 2013). NIST Real Gas model was used to get the properties of CO_2. Pressure-based coupled algorithm was chosen for the pressure-velocity coupling method. When the iterative residuals of the governing equations are less than 10^{-5} and the monitoring values of the area-weighted average temperature at the outlet are stable, the numerical simulation is considered converged.

3.3 Mesh independency

Structured meshes of the analysis domains are generated using ANSYS ICEM 18.1 as shown in Fig.2. Mesh sizes of 191232, 411846, and 587142 are used to check mesh independency. Table 1 shows the mean deviation of heat convection coefficient of all calculated points in Fig. 3, the relative error of the prediction data between case 2 and case 3 is quite small. Considering the computational cost and time, the number of 400,000 meshes are used as the baseline for the rest of the studies and the Near-wall Y+ of the study cases are controlled close to 1.

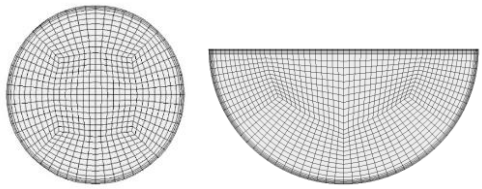

Fig. 2. Mesh models of cross section.

Table 1 Mesh independency study.

Cases	Number of cells	Near-wall Y+	Mean deviation from case 3
Case1	191232	1.7174343	2.43%
Case2	411846	1.1045907	0.45%
Case3	587142	0.90082807	0%

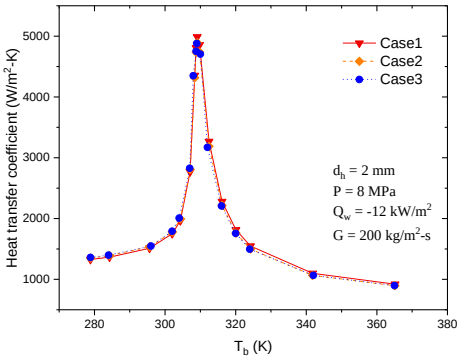

Fig. 3. Comparison of calculated heat transfer coefficient with different meshes.

3.4 Verification with experimental data

To verify the accuracy of the numerical simulation, the results of the numerical simulation are compared with the experimental data in (Dang and Hihara 2004) for the cooling process and with the experimental data in (Douglas and Olson 1998) for the heating process. The simulation model and boundary conditions are consistent with the experiment shown in Fig.3 and Fig.4. In this paper,

the heat transfer coefficients of the CFD data are calculated by Eq. (1).

$$h = \frac{Q_w}{T_w - T_b} \tag{1}$$

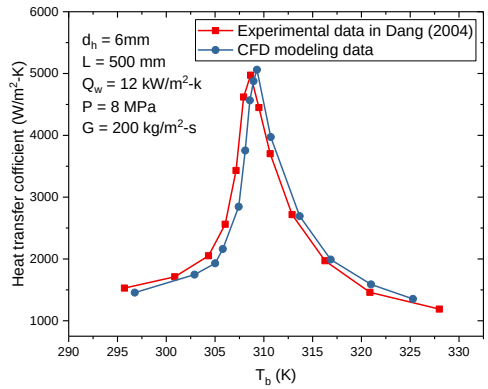

(a) Cooling case

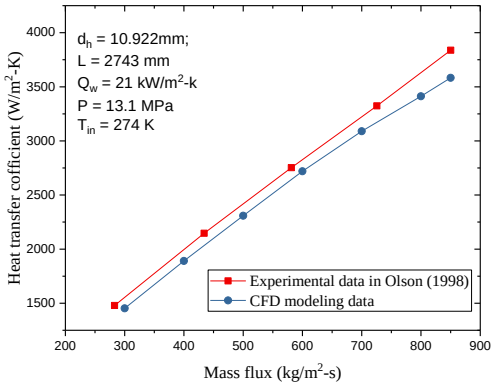

(b) Heating case

Fig. 4. Comparison between CFD results and experimental data of the circular channel.

Figure 4 (a) shows the comparison between the numerical analysis and experimental results of the circular channel for cooling process. The CFD data and experimental data maintain a good consistency when the bulk temperature is far away from the pseudocritical point. When T_b nears the critical point, the deviation increases. For the maximum point, the corresponding T_b of CFD result is 0.6 K larger than the experimental data, and the maximum heat transfer coefficient value of CFD data is also 3% larger than the experimental result. Figure 4 (b) shows the comparison between the numerical analysis and experimental results of the circular channel for the heating process. In Fig.4 (b), the heat transfer coefficients are expressed as a function of mass flux, and the inlet temperature (274 K) is very low, which makes T_b obviously far away from the T_m under the working pressure 13.1 MPa. This is not a comparison result with a wide T_b coverage, especially not covering the case near the pseudocritical point, however it covers multiple mass flux data points. As shown in Fig. 4, the relative error of the heat transfer coefficient value between experimental and CFD data is less than 10%.

Figures 5(a) and (b) show the comparison between the numerical analysis and experimental results of the semicircular channel in the cooling and heating cases with the T_b covering the pseudocritical point. The comparison results show that CFD data and experimental data maintain a good consistency in the heat transfer coefficient changing trend, and the maximum relative errors of the heat transfer coefficients in both cooling and heating cases are less than 20%.

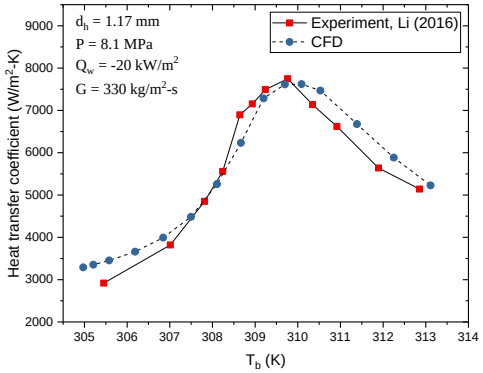

(a) Cooling case

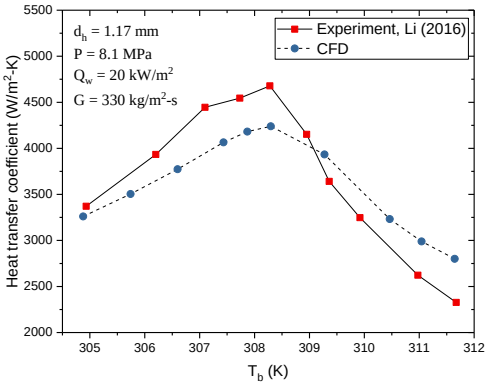

(b) Heating case

Fig. 5. Comparison between CFD results and experimental data of semicircular channel.

4. RESULTS AND ANALYSIS

4.1 Correlation for prediction of heat transfer coefficient

Most of the supercritical and pseudocritical heat transfer researchers have investigated the accuracy of established heat transfer correlations of circular pipe for cooling and heating process. Table 2 summarizes several widely used correlations to predict the in-tube supercritical CO2 heat transfer performance.

Gnielinski correlation (Gnielinski 1976) is widely used to predict single-phase fluids where the thermophysical properties are either constant or weakly varying. The Petukhov correlation (Petukhov 1970) was developed for determining the fluid Nusselt number with accounting for the variations of the viscosity, thermal conductivity, and specific heat. The Jackson correlation (Jackson and Hall 1979)

Table 2 Correlations of in-tube supercritical CO_2 used in comparisons to computational data.

Author/year	Correlations	Relevant factors
Gnielinski, 1976	$Nu = \frac{(f/8)(Re_b - 1000)Pr_b}{1.07 + 12.7\sqrt{\frac{f}{8}}(Pr_b^{\frac{2}{3}} - 1)}[1 + (\frac{d}{L})^{2/3}]$	$f = [1.82\log_{10}(Re_b) - 1.64]^{-2}$
Petukhov, 1961	$Nu_b = Nu_{ob}(\frac{\mu_b}{\mu_w})^{0.11}(\frac{k_b}{k_w})^{-0.33}(\frac{\overline{C_P}}{C_{pb}})^{0.35}$	$\overline{C_P} = \frac{i_b - i_w}{T_b - T_w}$ $Nu_{ob} = \frac{(f/8)Re_bPr_b}{1.07 + 12.7\sqrt{\frac{f}{8}}(Pr_b^{\frac{2}{3}} - 1)}$ $f = [0.79(Re_b) - 1.64]^{-2}$
Jackson, 1979	$Nu = 0.0183Re_b^{0.82}Pr_b^{0.5}(\frac{\rho_w}{\rho_b})^{0.3}(\frac{\overline{C_P}}{C_{pb}})^n$	$T_b < T_w < T_m$ or $1.2T_m < T_b < T_w$: n=0.4 $T_b < T_m < T_w$: $n = 0.4 + 0.2(\frac{T_w}{T_m} - 1)$ $T_m < T_b < 1.2T_m$, and $T_b < T_w$: $n = 0.4 + 0.2\left(\frac{T_w}{T_m} - 1\right)[1 - 5\left(\frac{T_b}{T_m} - 1\right)]$
Olson, 1998	$Nu = Nu_{PG}(\frac{\rho_w}{\rho_b})^{0.3}(\frac{\overline{C_P}}{C_{pb}})^n$	$\overline{C_P} = \frac{i_b - i_w}{T_b - T_w}$ $\frac{T_w}{T_m} < 1$, or $\frac{T_b}{T_m} \geq 1.2$: $n = 0.4$ $T_b / T_m < 1 \leq T_w / T_m$: $n = 0.4 + 0.18(\frac{T_w}{T_m} - 1)$ $\frac{T_w}{T_{pc}} \geq 1$, or $1 < \frac{T_b}{T_{pc}} < 1.2$: $n = 0.4 + 0.18\left(\frac{T_w}{T_m} - 1\right)[1 - 5\left(\frac{T_b}{T_m} - 1\right)]$ $Nu_{PG} = \frac{(f/2)(Re_b - 1000)Pr_b}{1 + 12.7\sqrt{\frac{f}{2}}(Pr_b^{\frac{2}{3}} - 1)}[1 + (\frac{d}{L})^{2/3}]$ $\frac{1}{\sqrt{f}} = \log_{10}\left(Re\sqrt{f}\right) - 0.4$

used the density ratios between the wall and bulk conditions and a heat capacity ratio to account for the rapid variations in density and heat capacity when T_b and T_w are near the pseudocritical point, especially in conditions of large heat fluxes. The Jackson correlation has been studied by (Ghajar and Asadi 1986) and concluded as the most accurate one to predict the heat transfer coefficient in the supercritical region. The Olson correlation (Douglas and Olson 1998) used the Gnielinski correlation as the basis for the modified method similar to Jackson correlation, and this correlation was verified with heat transfer experiment data of turbulent SCO_2 in heated horizontal tubes.

4.2 Comparison of correlation prediction and CFD data for circular channel

Figure 6 shows comparisons between the prediction models and the CFD data of a 6mm hydraulic diameter circular channel at a Q_w of -12 kW/m^2, G of 200 kg/m^2-s and outlet pressure of 8 MPa for the cooling process. As shown in Fig. 6(a), the maximum value of Gnielinski correlation occurs at the point T_b=T_m.

The maximum value of CFD prediction appears at the position where T_b is slightly larger than T_m. It is because that the thermosphysical properties of the fluids near the channel wall, which are determined by the local wall temperature, T_w, are not being considered in Gnielinski correlation. The fluid properties near the wall also significantly affect the heat transfer performance in addition to the fluid properties of the core region. As T_w < T_b for the cooling case, the maximum values of the specific heat capacity and thermal conductivity of the fluid near the wall will occur at the position of T_b slightly larger than T_m, which makes the maximum heat transfer coefficient occurs at the point where T_b > T_m. Olson and Jackson correlations both consider the influence of the near-wall fluid thermophysical

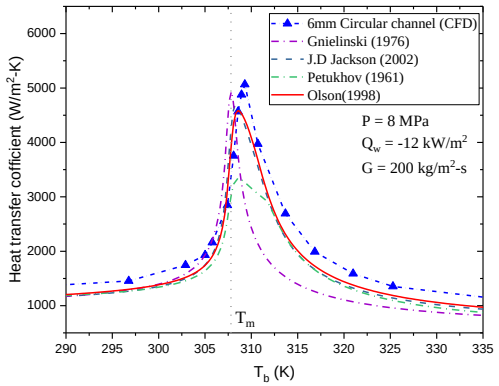

(a) Heat transfer coefficient

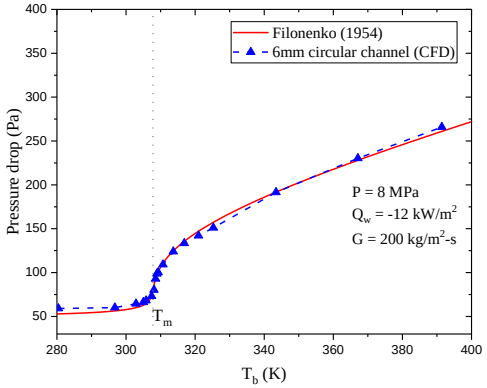

(b) Pressure drop

Fig. 6. Comparison between prediction models and CFD data for cooling process.

parameters on the heat transfer intensity and give a more reasonable prediction. When T_b gets far away from T_m, the influence of fluid temperature on the thermophysical parameters gradually weakens, and the relative deviation of the prediction results among the correlations are also gradually decreases. As for the pressure drops shown in Fig. 6(b), Filonenko equation provides well predictions of the CFD data under this cooling process.

Figure 7 shows comparisons between the prediction models and the CFD data of a 6 mm hydraulic diameter circular channel at a Q_w of 12 kW/m^2, G of 200 kg/m^2-s and outlet pressure of 8 MPa for the heating process. As shown in Fig.7(a), significant prediction errors of the Gnielinski correlation happen near the pseudocritical point. This means that the near-wall thermophysical properties of the SCO_2 fluid have a greater effect on its convective heat transfer performance under heating conditions. As for the heating cases, $T_w > T_b$, the dynamic viscosity and fluid density near the wall are less than the corresponding core region parameters. While the changes of the thermal conductivity and specific heat capacity of the near-wall fluid depend on the relationship among T_w, T_b, and T_m. As a result, the correlation should be a piecewise function based on the relationship among T_w, T_b, and T_m and include the modification of the near-wall parameter. Figure 7 (a) shows that Olson and Jackson correlation with this correction method has higher accuracy. As to the pressure drop, the Filonenko equation gives well predictions as $T_b < T_m$, and when $T_b > T_m$, there is about 10% error between Filonenko equation and the CFD data for this heating process.

According to the analysis in this section, Olson correlation has a more reasonable prediction for the heat transfer coefficients of SCO_2 in this 6 mm circular channel compared to the other three correlations for both cooling and heating process. For pressure drop, the Filonenko correlation shows a well applicability for both in-tube cooling and heating cases.

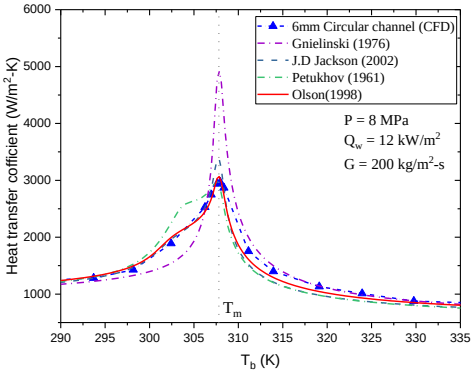

(a) Heat transfer coefficient

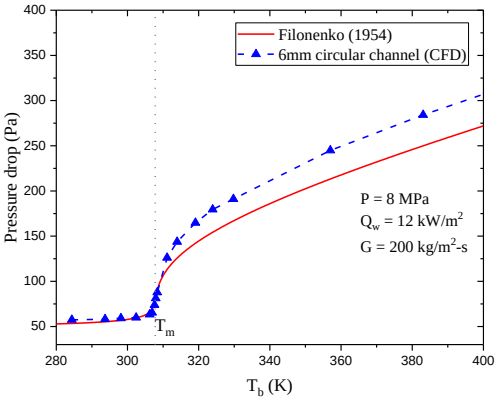

(b) Pressure drop

Fig. 7. Comparison between prediction models and CFD data for heating process.

4.3 Comparison of circular and semicircular channels

Figure 8 shows a comparison between the circular channel and the semicircular channel of 6 mm hydraulic diameter for the cooling process at a Q_w of ±12 kW/m^2, G of 200 kg/m^2-s and outlet pressure of 8 MPa. As shown in Fig. 8(a), the heat transfer coefficients of the semicircular channel are relatively smaller than those of the circular channel but not significant for the cooling process. While for the heating process, as Fig. 8(b) shown, the heat transfer coefficients of the semicircular channel are significantly smaller than those of the circular channel. This means that the cross-sectional shape of the channel has a significant effect on the heat transfer coefficient even at the same hydraulic

diameter and boundary condition for the heated channel.

Figure 9 shows the fluid velocity plots of the cross-section for both circular and semicircular channels. The figure shows that the corner area of the semicircular channel has an obvious blocking effect on the nearby fluid. As a result, the velocity of the fluid around the corner area decreases and the local heat transfer is weakened, which makes the heat transfer intensity in the corner region significantly weaker than that in the non-corner region. This is the reason that the average heat transfer coefficient of the semicircular channel is lower than that of the circular channel. Therefore, the empirical formula based on circular channel needs to be modified so that it can be used to predict the heat transfer characteristics of the semicircular channel.

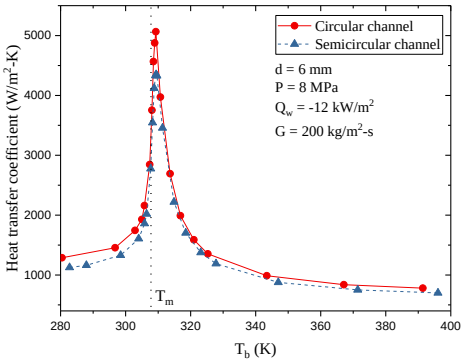

(a) Cooling case

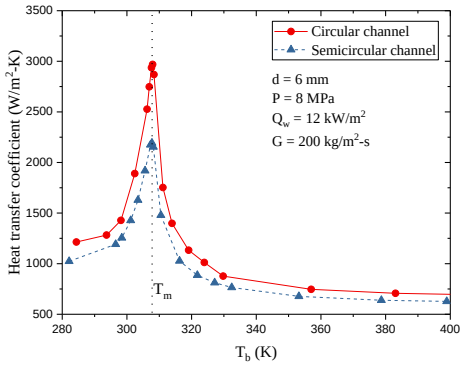

(b) Heating case

Fig. 8. Comparison between circular and semicircular.

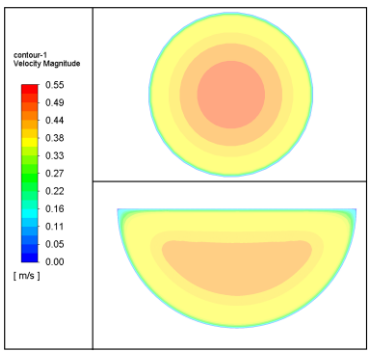

Fig. 9. Fluid velocity contour plot of channel cross section.

4.4 Comparison of correlation prediction and CFD data for semicircular channel

Figure 10 shows a comparison between the prediction models and the CFD data for a 6 mm hydraulic diameter semicircular channel at Q_w of ±12 kW/m^2, G of kg/m^2-s and outlet pressure of 8 MPa for cooling and heating process. As shown in Fig. 10(a), all of these models show relatively reasonable predictions of the CFD data as T_b is much higher or lower than T_m in both cooling and heating cases. Whereas as the T_b nears the T_m, Olson and Jackson correlations show relatively well prediction of the CFD data for the cooling process. In addition, the predictions of the Olson correlation are relatively closer to the CFD data for the cooling process.

However, for the heating process, none of these correlations gives a reasonable prediction of the heat transfer coefficients of the semicircular channel when T_b nears the T_m as shown in Fig. 10 (b). Whereas when T_b is much larger or lower than T_m, these four correlations can provide relative reasonable predictions, for the reason being in these conditions the CO_2 fluid thermal physical properties are weakly varying.

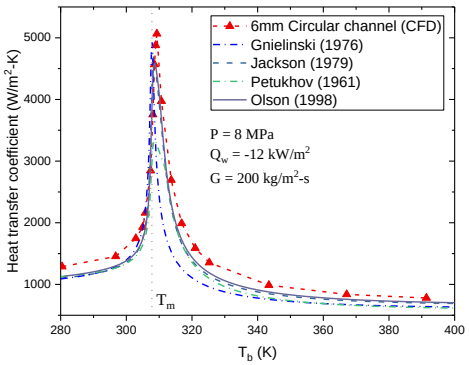

(a) Cooling cases

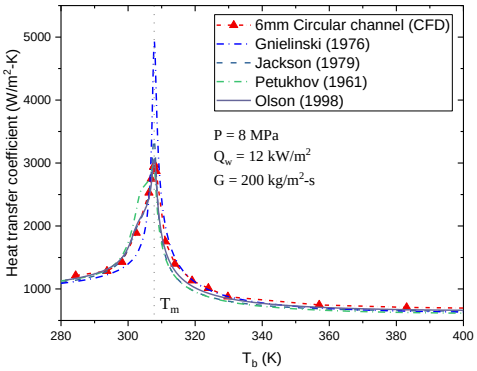

(b) Heating cases

Fig. 10. Comparison of the prediction models and the CFD data of semicircular channel.

4.5 Modified prediction correlation of heated semicircular channel

It can be seen from Sections 4.3 and 4.4, for the heating process, even if the hydraulic diameter is the

same, the heat transfer coefficient of the semicircular channel is significantly smaller than that of the circular channel, and the prediction correlation of the circular channel is not applicable any more. It means that using hydraulic diameter as the length scale to define dimensionless parameters cannot ensure the similarity between the circular and semicircular channels. Geometry based modifications need to be taken into account in the formula. The viscosity of the fluid also has a significant influence on the local heat transfer performance, especially at the conner area. Therefore, a correction term μ_w/μ_b should also be added into the correlation to modify the influence of the viscosity of the fluid.

Modified model was proposed with correction terms for the viscosity and geometric parameters based on Olson correlation to predict the heat transfer coefficient for the heating process of the semicircular channels in this study as shown in the following Eq. (2) to Eq. (6).

$$\mathrm{Re}_{\sqrt{A}} = \rho v \sqrt{A} / \mu \tag{2}$$

Then $\mathrm{Re}_{\sqrt{A}}$ is used to calculate the friction factor $f_{\sqrt{A}}$:

$$\frac{1}{\sqrt{f_{\sqrt{A}}}} = \log_{10}\left(\mathrm{Re}_{\sqrt{A}}\sqrt{f_{\sqrt{A}}}\right) - 0.4 \tag{3}$$

$$Nu_{semi} = \mathrm{Nu}_{PG}\frac{0.9d}{\sqrt{A}}\left(\frac{\rho_w}{\rho_b}\right)^{0.3}\frac{\overline{C_P}}{C_{pb}})^n(\frac{\mu_w}{\mu_b})^{0.07} \tag{4}$$

$$h = Nu_{semi} * k / \sqrt{A} \tag{5}$$

Where $\overline{C_P}$ and the constant n were calculated as Table 2 shown. And Nu_{PG} was calculated as in Douglas and Olson 1998 using $\mathrm{Re}_{\sqrt{A}}$ and $f_{\sqrt{A}}$ as Eq. (6):

$$\mathrm{Nu}_{PG} = \frac{(f_{\sqrt{A}}/2)(\mathrm{Re}_{\sqrt{A}} - 1000)\mathrm{Pr}_b[1+(\frac{d}{L})^{2/3}]}{1+12.7\sqrt{\frac{f_{\sqrt{A}}}{2}}(\mathrm{Pr}_b^{\frac{2}{3}}-1)} \tag{6}$$

The following analysis will study the heat transfer characteristics and the applicability of this modified model for the heated semicircular channel of SCO_2 in different hydraulic diameters, mass flux, heat flux and operating pressure conditions.

4.6 Effect of boundary condition and verification of the modified correlation model

(1) Effect of hydraulic diameter

Figure 11 shows the effect of hydraulic diameter on heat transfer coefficients at P = 8 MPa, Q_w = ±12 kW/m^2 and G = 200 kg/m^2-s. The heat transfer coefficient increases with the decrease of the channel hydraulic diameter for both cooling and heating process. However, the influence of the pipe diameter on the heat transfer coefficients is not significant for both heating and cooling conditions.

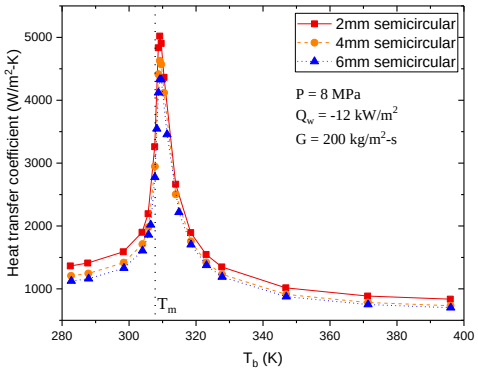

(a) Cooling case

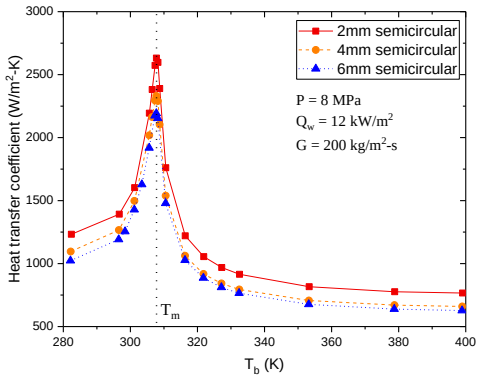

(b) Heating case

Fig. 11. Effect of hydraulic diameter on heat transfer coefficient.

Figures 12(a), (b) and (c) show comparisons of Olson correlation, modified model and the CFD data at P = 8 MPa, G = 200 kg/m^2-s, Q_w = 12 kW/m^2 for various channel hydraulic diameters (d = 2, 4 and 6 mm). The comparison results show that the modified model has better prediction results than the Olson correlation for semicircular channels with the three diameter sizes, especially when T_b is near T_m.

(2) Effect of heat flux Q_w

Figure 13 shows the effect of Q_w on the heat transfer coefficients of a 2 mm diameter semicircular channel at P = 8 MPa, G= 400 kg/m^2-s for various Q_w (6, 12 and 18 kW/m^2). As shown in Fig.13, the heat transfer coefficients decrease significantly with the increase of the wall heat flux when T_b nears T_m. When T_b is much larger or much smaller than T_m, the impact of Q_w on the heat transfer coefficient becomes very weak. Such results can be understood by accounting for the relatively slow changes in the CO_2 thermo-physical properties when the value of T_b is much larger or much smaller than T_m.

Figures 14(a), (b) and (c) provide comparisons of the modified Olson model prediction results with CFD data under three different heat fluxes 6, 12, and 18 kW/m^2. It can be seen from the comparisons that the modified model gives a reasonable prediction of heat

transfer coefficients from CFD model under various heat flux values.

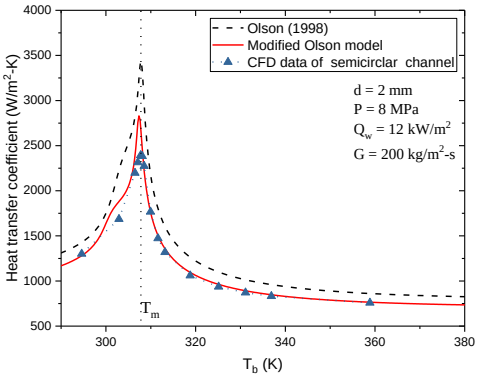

(a) d = 2 mm

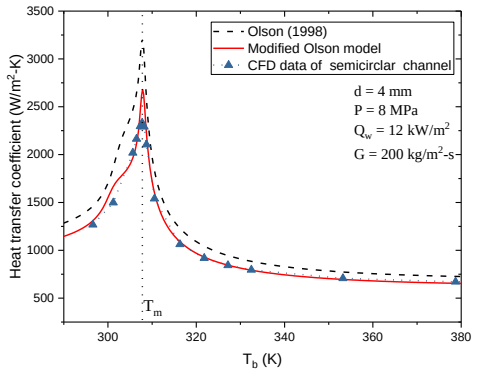

(b) d = 4 mm

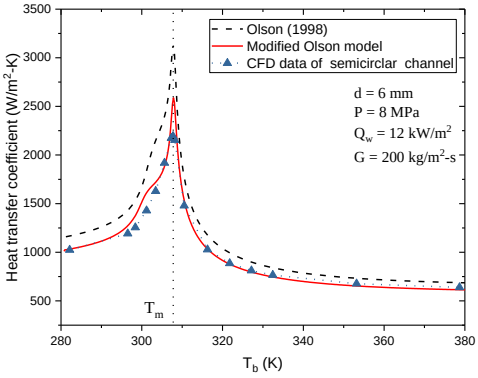

(c) d = 6 mm

Fig. 12. Verification of the modified correlation for heating process at different d.

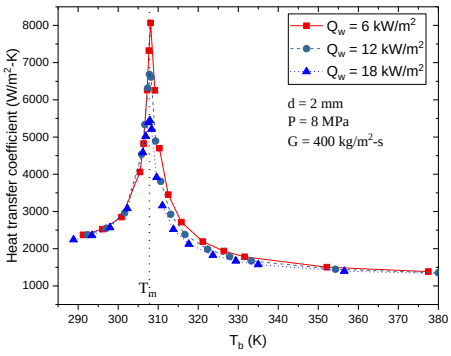

Fig. 13. Effect of heat flux on heat transfer coefficient in heating case.

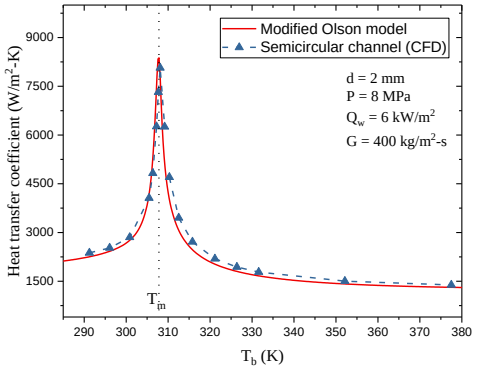

(a) Q_w = 6 kW/m^2

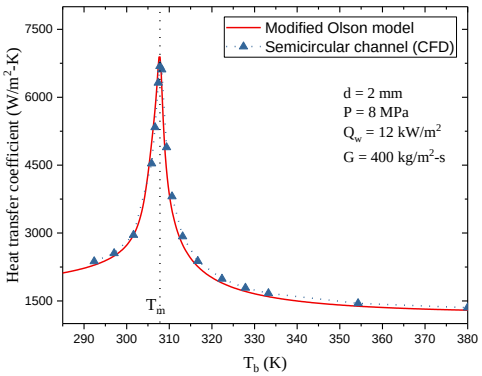

(b) Q_w = 12 kW/m^2

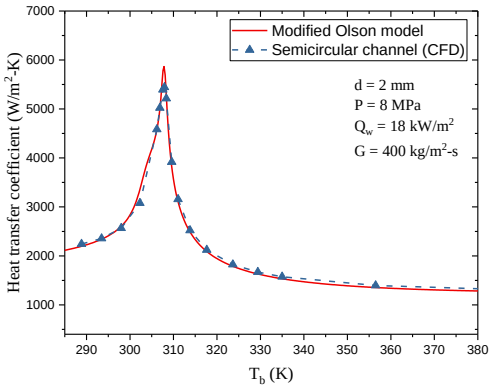

(c) Q_w = 18 kW/m^2

Fig. 14. Verification of the modified correlation at different Q_w.

(3) Effect of mass flux G

Figure 15 shows the effect of mass flux on the heat transfer coefficients of the 2 mm hydraulic diameter semicircular channel at P = 8 MPa, Q_w = 12 kW/m^2 and G = 200, 400 and 600 kg/m^2-s. As this figure shown, the heat transfer coefficient increases as the increasing of mass flux. Because the increased G causes the increase of mass average velocity of the CO_2 fluid, which will also lead to an increase in the fluid Re.

As the inlet mass flux significantly impacts the heat transfer coefficient of the in-tube SCO_2 fluid, comparisons of the modified Olson correlation and CFD results were conducted with different mass fluxes including 200, 400, and 600 kg/m^2-s. As 200 and 400 kg/m^2-s cases have already shown in the Fig.

12 and Fig. 14. The Fig. 16 only provides the case of 600 kg/m^2-s. It can be seen from all these figures that the modified correlation can provide well prediction of the heat transfer coefficients of SCO_2 in the heated semicircular channel with different mass flux ranging.

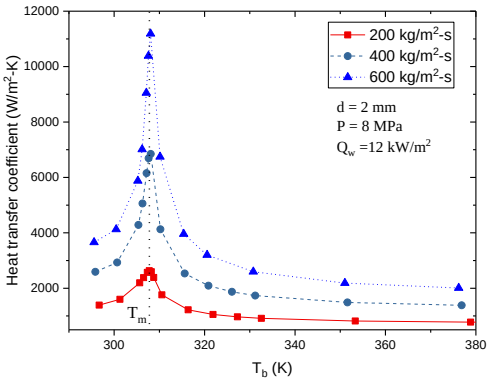

Fig. 15. Effect of G on the heat transfer coefficient in heating case.

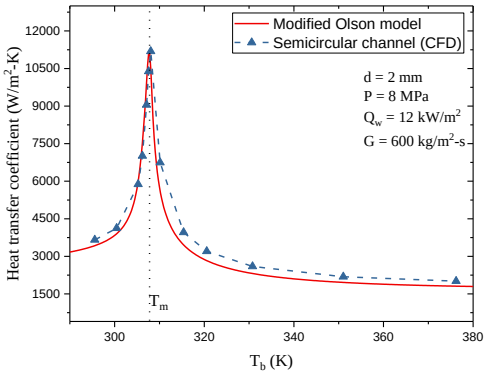

Fig. 16. Verification of the modified correlation at G = 600 kg/m^2-s.

(4) Effect of working pressure

Figure 17 shows the heat transfer coefficients for d = 2 mm, G = 200 kg/m^2-s, Q_w=12 kW/m^2 and different outlet pressure (P = 7.5, 8, and 9 MPa). As shown in this figure, the maximum heat transfer coefficient occurs approximately, where $T_b = T_m$. When T_b is near T_m, the heat transfer coefficient strongly depends on P. As P increased from 7.5 MPa to 9 MPa, the maximum heat transfer coefficient decreased from 8277 W/m^2-k to 4780 W/m^2-k. However, when T_b is far away from T_m, the heat transfer coefficients tend to be equal and show the independence of P. This is because when T_b is far away from T_m, the thermal properties of SCO_2 are little affected by the changing of pressure as Fig. 1 shown.

As the operating pressure significantly impacts the heat transfer coefficient of the in-tube SCO_2 fluid near the pseudocritical point, comparisons of the modified Olson correlation and CFD results were conducted in different outlet pressure 7.5, 8 and 9 MPa. As can be seen from Fig. 18 (8 MPa case has already been provided in Fig. 12), the modified correlation model gives a reasonable prediction of the heat transfer coefficients of SCO_2 in the heated semicircular channel with different operating pressure ranging.

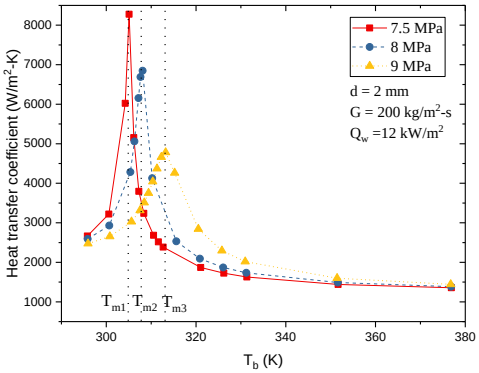

Fig. 17. Effect of operating pressure on heat transfer coefficient in heating case.

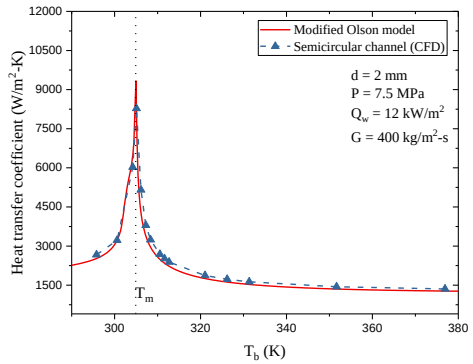

(a) P = 7.5 MPa

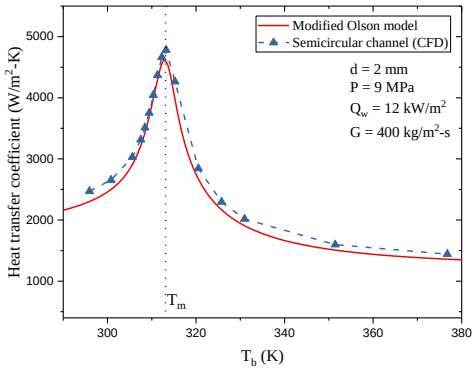

(a) P = 9 MPa

Fig. 18. Verification of the modified correlation at different P.

5. CONCLUSION

Comparative study of heat transfer of SCO_2 in horizontal circular and semicircular channels for both cooling and heating process was investigated based on experimentally verified CFD models. CFD results were compared with several existing correlations, and a modification based on Olson correlation was proposed to predict the heat transfer coefficients of the semicircular channel for the

heating process. The main conclusions of this study are summarized as follows:

For the cooling process, the heat transfer coefficients of semicircular channel are slightly smaller than those of the circular channel under the same boundary and hydraulic diameter, but the deviation is not significant. Olson correlation provides good predictability for both circular and semicircular channels.

For the heating process, the heat transfer coefficient of SCO_2 in the semicircular channel is significantly smaller than that of the circular channel. Olson correlation still has well prediction for the circular channel for heating process. As for the semicircular channel, the predicted value of this correlation has a significant deviation.

A modified model was proposed based on the Olson correlation to predict the heat transfer coefficient of SCO_2 in the semicircular channel for heating process. This modified correlation is verified with the CFD data in different channel hydraulic diameter, heat flux, mass flux, and operating pressure, the comparison results show that the modified model can well predict the heat transfer coefficient of SCO_2 in the semicircular channel.

ACKNOWLEDGEMENTS

This project is supported by the Fund of Natural Science Project of Hunan Province, China, with the item number 2020JJ5393.

Education Department of Hunan Province, China, with the item number 18C0735.

REFERENCES

Cabeza, L. F., A. de Gracia, A. I. Fernández and M. M. Farid (2017). Supercritical CO2 as heat transfer fluid: A review. *Applied Thermal Engineering* 125, 799–810.

Chen, M., X. Sun, R. N. Christensen, S. Shi, I. Skavdahl, V. Utgikar and P. Sabharwall (2016). Experimental and numerical study of a printed circuit heat exchanger. *Annals of Nuclear Energy* 97, 221–231.

Dang, C. and E. Hihara (2004). In-tube cooling heat transfer of supercritical carbon dioxide. Part 2. Comparison of numerical calculation with different turbulence models. *International Journal of Refrigeration* 27(7 SPEC. ISS.), 748–760.

Douglas, A. and D. A. Olson, (1998). *Heat Transfer in Turbulent Supercritical Carbon Dioxide Flowing in a Heated Horizontal Tube . NISTIR 6234*.

Figley, J., X. Sun, S. K. Mylavarapu and B. Hajek (2013). Numerical study on thermal hydraulic performance of a Printed Circuit Heat Exchanger. *Progress in Nuclear Energy* 68, 89–96.

Ghajar, A. J. and A. Asadi (1986). Improved forced convective heat-transfer correlations for liquids inthe near-critical region. *AIAA Journal* 24(12), 2030–2037.

Gnielinski, V. (1976). New Equations for Heat and Mass Transfer in Turbulent Pipe and Channel Flow. *International Chemical Engineering*.

Jackson, J. D. and W. B. Hall (1979). Influences of Buoyancy on Heat Transfer To Fluids Flowing in Vertical Tubes under Turbulent Conditions. *Institution of Mechanical Engineers, Conference Publications*.

Kim, J. H., S. Baek, S. Jeong and J. Jung (2010). Hydraulic performance of a microchannel PCHE. *Applied Thermal Engineering* 30(14–15), 2157–2162.

Kim, T. H., J. G. Kwon, S. H. Yoon, H. S. Park, M. H. Kim and J. E. Cha (2015). Numerical analysis of air-foil shaped fin performance in printed circuit heat exchanger in a supercritical carbon dioxide power cycle. *Nuclear Engineering and Design* 288, 110–118.

Kruizenga, A., H. Li, M. Anderson and M. Corradini (2012). Supercritical carbon dioxide heat transfer in horizontal semicircular channels. *Journal of Heat Transfer* 134(8).

Lee, S. M., and K. Y. Kim (2013). Comparative study on performance of a zigzag printed circuit heat exchanger with various channel shapes and configurations. *Heat and Mass Transfer/Waerme- Und Stoffuebertragung* 49(7), 1021–1028.

Li, H., A. Kruizenga, M. Anderson, M. Corradini, Y. Luo, H. Wang and H. Li (2011). Development of a new forced convection heat transfer correlation for CO2 in both heating and cooling modes at supercritical pressures. *International Journal of Thermal Sciences* 50(12), 2430–2442.

Li, H., Y. Zhang, L. Zhang, M. Yao, A. Kruizenga and M. Anderson (2016). PDF-based modeling on the turbulent convection heat transfer of supercritical CO2 in the printed circuit heat exchangers for the supercritical CO2 Brayton cycle. *International Journal of Heat and Mass Transfer* 98, 204–218.

Meshram, A., A. K. Jaiswal, S. D. Khivsara, J. D. Ortega, C. Ho, R. Bapat and P. Dutta (2016). Modeling and analysis of a printed circuit heat exchanger for supercritical CO 2 power cycle applications. *Applied Thermal Engineering* 109, 861–870.

Mylavarapu, S., X. Sun, J. Figley, N. Needler and R. Christensen (2009). Investigation of high-temperature printed circuit heat exchangers for very high temperature reactors. *Journal of Engineering for Gas Turbines and Power* 131(6), 1–7.

Nikitin, K., Y. Kato and L. Ngo (2006). Printed circuit heat exchanger thermal-hydraulic

performance in supercritical CO2 experimental loop. *International Journal of Refrigeration* 29(5), 807–814.

Petukhov, B. S. (1970). Heat Transfer and Friction in Turbulent Pipe Flow with Variable Physical Properties. *Advances in Heat Transfer* 6; 503-564

Pitla, S. S., D. M. Robinson, E. A. Groll and S. Ramadhyani (1999). Heat transfer from supercritical carbon dioxide in tube flow: a critical review. *ASHRAE Transactions 105*(May 2013), 37–41.

Rao, N. T., A. N. Oumer and U. K. Jamaludin (2016). State-of-the-art on flow and heat transfer characteristics of supercritical CO2 in various channels. *Journal of Supercritical Fluids* 116, 132–147.

Tsuzuki, N., Y. Kato and T. Ishiduka (2007). High performance printed circuit heat exchanger. *Applied Thermal Engineering* 27(10), 1702–1707.